



Cite this: DOI: 10.1039/d1dt00033k

Quenchable amorphous glass-like material from
VF₃[†]Raimundas Sereika,^{id} *^{a,b} Sooran Kim,^c Takeshi Nakagawa,^{id} ^a Hirofumi Ishii,^d
Yang Ding*^a and Ho-kwang Mao^aHPSTAR
1168-2021

The quite simple but relatively stable VF₃-type compounds are known to be of major interest due to their building blocks – octahedra that are extremely important in perovskites as well. Here, we show that the VF₆ octahedron in VF₃ varies over a fairly wide pressure range (0–50 GPa), maintaining undisturbed rhombohedral crystal symmetry. Half of this pressure, VF₆ rotates easily while the other undergoes strong uniaxial deformation in a “super-dense” condition. The congested sphere packing ultimately does not endure and drives the material to amorphize. We observed that the amorphous state could be quenched and acquire a transparent glass-like appearance when unloaded to ambient conditions. Dramatic, pressure-induced changes are clarified by phonon dispersion curves with the imaginary phonon mode, the so-called phonon soft mode, which indicates the structural instability. The distortion of the VF₆ octahedra is attributed to the distinctive amorphization that could be further searched for throughout the whole almost identical VF₃-type series providing metal trifluorides of various amorphous species.

Received 4th January 2021,
Accepted 27th January 2021

DOI: 10.1039/d1dt00033k

rsc.li/dalton

Introduction

Vanadium trifluoride (VF₃) is a prototypic compound whose structure is adopted by many metal trifluorides (composition MF₃ where M = Al, Cr, Fe, Ga, Ti, etc.).^{1–8} The metal ion is surrounded by an octahedron of corner-shared fluorine atoms. The octahedral framework is the same as in the idealized perovskite-type structure AMX₃ in which the A site is vacant. Structural affinities are gaining importance in studying materials under extreme conditions, as specific features may recur. There are several intriguing phenomena highlighted as recurrent or highly expected in the MF₃ series, such as Jahn-Teller and spin-orbit coupling, and giant barocaloric effects.^{4–7} Here, the octahedral MF₆ plays a very important role in terms of temperature or pressure. Many MF₃ compounds are cubic (*Pm* $\bar{3}$ *m*) in the high-temperature phase and become rhombohedral (*R* $\bar{3}$ *c*) at room temperature by rotations of octahedra around their three-fold axes.^{8,9} The behavior under high pressure is also implicit as it is known that the coupled MX₆

octahedra rotate readily *via* the application of hydrostatic pressure, thereby reducing the unit-cell volume.^{2,3,10,11} The stability of the rhombohedral MF₃ compounds is quite remarkable because, to the best of our knowledge, no structural transitions are reported, although one example of amorphization was found at pressures higher than 50 GPa.¹¹ The latter transition occurs in iron trifluoride (FeF₃) and is claimed to be of the first order with a high-energy barrier.

In this work, we found that analogous VF₃ also undergoes transitions to the amorphous state at similar pressures. It manifests quite vividly and may have significant implications for the design of novel materials as we observe that the amorphous phase is quenchable, providing a transparent glass-like form. Surprisingly, the whole process takes place at room temperature and without the use of rapid compression/unloading¹² or other aids except the conventional diamond-anvil cell (DAC)¹³ alone. Therefore, we focus on the discovered amorphization, its nature, possible distinctions, and similarities in the VF₃-type family.

Experimental and computational
methods

The VF₃ samples used in the present work were obtained from Alfa Aesar (stock no. 81115). Initially, the quality was tested by laboratory powder X-ray diffraction (XRD) analysis with a PANalytical Empyrean diffractometer (Cu K α radiation) (see Fig. S1[†]). Then, several symmetric DACs with 200, 300, and

^aCenter for High Pressure Science and Technology Advanced Research, Beijing 100094, China. E-mail: yang.ding@hpstar.ac.cn

^bVytautas Magnus University, K. Donelaičio Str. 58, Kaunas 44248, Lithuania. E-mail: raimundas.sereika@vdu.lt

^cDepartment of Physics Education, Kyungpook National University, Daegu 41566, Korea

^dNational Synchrotron Radiation Research Center, Hsinchu 30076, Taiwan

[†]Electronic supplementary information (ESI) available. See DOI: 10.1039/d1dt00033k

400 mm culets were employed to apply pressure. Stainless steel and rhenium gaskets were used for pressures below and above 50 GPa, respectively. The sample, together with a ruby sphere and gas (use of neon or helium gas showed no noticeable difference) as a pressure medium, were all loaded into the prepared chamber within the gasket. The pressure was measured *via* the ruby fluorescence method.¹⁴

The *in situ* high-pressure XRD measurements were carried out using synchrotron radiation at the beamline BL12B2 of the SPring-8 (Hyogo, Japan). The experiments were performed several times in an angle-dispersive mode. Each time, the wavelength of the X-rays was calibrated using a CeO₂ standard. The two-dimensional digitalized diffraction patterns were integrated into one-dimensional profiles, and the peak positions were semi-automatically determined at a certain azimuth angle using IPAnalyzer and PDIndexer softwares.¹⁵ Rietveld refinements were carried out in EXPO2014.¹⁶

The high-pressure Raman spectra were measured using a MonoVista CRS + spectrometer with a 532 nm laser wavelength, which gave the best signal. The original S&I VistaControl v4.4.6 software was used to collect and process the data. The data collection time and laser power were maintained the same for each spectrum except for ambient pressure.

The computational study was carried out based on the first-principles density functional theory (DFT) approach using VASP software.¹⁷ We performed the spin-polarized calculations with ferromagnetic ordering in the framework of the DFT+*U* (*U* = 3.3 eV for the V *d* orbital¹⁸). The Perdew–Burke–Ernzerhof functional was employed as an exchange–correlation functional.¹⁹ To obtain reasonably stable structures of VF₃ under different pressures, the lattice parameters and internal atomic positions of the unit cell were fully relaxed until total residual forces were smaller than 10^{−2} eV Å^{−1}. PHONOPY²⁰ software was used for phonon calculations. The dynamical matrix was calculated with the finite displacement method using the 2 × 2 × 2 supercell with 4 × 4 × 4 *k*-point mesh. Using the 2 × 2 × 2 supercell, Γ , F, T, and L are exact points in the Brillouin zone.

Results and discussion

The pressure dependences of the lattice parameters and volume reduction of VF₃ under high pressure are shown in Fig. 1a–c. The behavior in the range of 0–30 GPa is akin to the measurements of other VF₃-type materials.^{2,3,11,21} In VF₃, we observed a noticeable increase of 0.46% in the lattice parameter *c* at 4.95 GPa (see Fig. 1b). The elongation phenomenon of the *c*-axis is explained by the increasing octahedral strain at elevated pressures.^{3,21,22} Long ago, it was found that this strain originates from repulsive interactions between the cations.² Since the MF₆ octahedra in these compounds contain two independent F–F distances, one within and another outside the basal plane, the F–F distance within the basal plane decreases more than the out-of-plane F–F distance at elevated

pressure, thereby elongating the MF₆ along the *c*-axis. The experimentally estimated value of 0.46% for VF₃ is comparable with increases for GaF₃ (0.26% at 3.5 GPa),³ FeF₃ (0.62% at 4 GPa),³ CrF₃ (0.17% at 4 GPa),²¹ and TiF₃ (~3% at 5 GPa).²

The best fit of zero-pressure bulk modulus *B*₀ and its pressure derivative *B*'₀ yielded typical values of the MF₃ family. The bulk modulus for VF₃ is estimated to be *B*₀ = 19.4 GPa, and its first pressure derivative is *B*'₀ = 12.0 (see Fig. 1c). Such a bulk modulus confirms the fact that VF₃ is soft under high pressure. In turn, this supports that the compression process takes place by the bending of chemical bonds, in contrast to the direct compression of the chemical bonds, which usually gives much higher bulk moduli. In the MF₃ family, *B*₀ is known to be related to the ambient pressure unit-cell volume *V*₀.³ Fig. 1f shows that *B*₀ of VF₃ fits well to the scaling relation by Anderson and Nafe:²³

$$B_0 = K \cdot V_0^{-n}, \quad (1)$$

where *K* and *n* are constants for a given group of compounds. *K* depends, among other factors, on the valency and *n* on the nature of the chemical bond. We define the scaling exponent as *n* = 5.76 ± 0.7, which is similar to previous reports,³ but is still larger than the normally observed values for covalent and ionic compounds.²⁴

The so-called 8/3/*c*2 hexagonal sphere-packing model provides quite a reasonable description of the compression mechanism predominant in VF₃-type compounds up to the close-packed state, as the model is based on incompressible spheres.^{21,22} According to this model, which is characterized by the positional parameter *x* of the F atoms and lattice parameters (the only two factors which determine the geometric configuration of this structure), the limiting case is at *c/a* = 2.828 (or $\sqrt{3/3 \cdot c/a} = 1.633$) for *x* = 1/3.

The V atoms form no close-packed layers for 1/3 < *x* < 1/2 and close-packed layers for *x* = 1/3. The “super-densely” packed layers are formed for *x* < 1/3. We observe the value *c/a* = 2.828 is exceeded at a relatively low pressure of ~8 GPa (see Fig. 1d), but the *x* = 1/3 value is only reached at 18 GPa, meaning that VF₃ fails to comply with strict ideal packing. The difference is mainly the non-negligible volume of the partly interstitial V atoms among the F-atom sphere packing. Such a discrepancy in real cases is analyzed and discussed in detail in ref. 2. Further, compression proceeds with the fluoride ions arranged more and more densely, experiencing a “super-dense” sphere packing, until finally the system breaks down. Fig. 1e shows the mentioned close-packing states with reference to fluorine *x* coordinate dependence on the axial *c/a* ratio. The rotation of the octahedra as well as the volume reduction do not cease after the “super-dense” conditions are reached. They exist in the entire pressure range and are, therefore, consistent with the equation of state (EoS) fitted up to 30 GPa. Other studies have shown that the MX₆ octahedra remain almost undistorted, and the enhancement in density in relation to the close-packed *x* = 1/3 phase is achieved through the compression of groups of three F atoms.³ Calcite

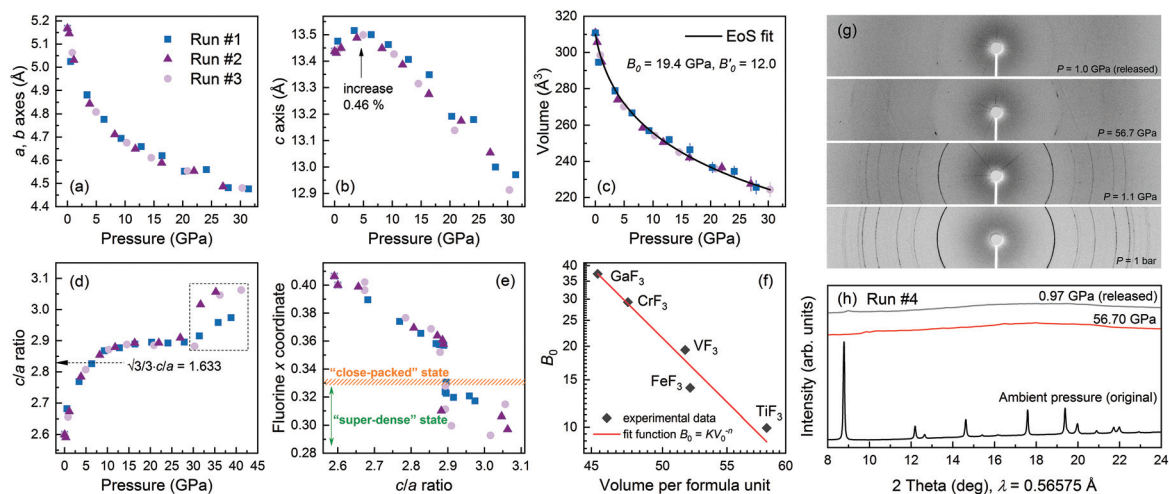


Fig. 1 Synchrotron XRD data for VF_3 powders. Pressure dependences of (a and b) lattice lengths, (c) unit-cell volume, and (d) the axial c to a ratio. The black curve is the calculated third-order Birch–Murnaghan EoS fit to the experimental data. The dashed area indicates the detachment points where the system rupture is occurring. (e) Positional parameter x of the F atoms in VF_3 versus the axial ratio c/a . (f) A log–log plot of the bulk modulus as a function of volume per formula unit for several MF_3 compounds. The red line represents the fit function, which is the scaling relation described in the text. (g and h) Portions of the diffraction images and patterns indicating quenchable amorphization.

(CaCO_3) is an example of such a compound as carbon is located between the three squeezed O atoms. However, later it was specified by other authors that this is only correct up to ~ 25 GPa.¹¹ At higher pressure, elongation of the octahedra was observed and was proven to be the dominant compression mechanism in this range as there is a mismatch between the unit-cell shape and rotation angle.

Our synchrotron XRD measurements indicate that the apparent intense diffraction peak broadening and intensity decrease in VF_3 take place from 30 to 45 GPa (details given in the ESI†). Thus, the data can be qualitatively evaluated up to a pressure of approximately 30 GPa. At higher pressures, the peaks continue to gradually disappear, leaving the pattern almost without peaks at 52–57 GPa (see Fig. 1g and h). Such behavior indicates amorphization and is in good agreement with the high-pressure measurements of FeF_3 ,¹¹ whereas TiF_3 and GaF_3 show a tendency similar to other VF_3 -type materials measured at lower pressures.^{2,3} Yet, we found that VF_3 has a tipping point, after which the amorphous state becomes locked. Depending on many factors, this point may be a little different. In our experiments, the lowest quenching pressure was 56.7 GPa.

To confirm quenchable amorphization, we performed optical Raman measurements. Fig. 2 shows the Raman spectra of VF_3 for various pressures. According to the space group in the rhombohedral ($R\bar{3}c$) phase, there are 14 normal optical modes of vibration at the center of the Brillouin zone:

$$\Gamma_{\text{opt}} = A_{1g} + 2A_{2g} + 3E_g + 2A_{1u} + 2A_{2u} + 4E_u. \quad (2)$$

Out of them, four Raman-active modes are expected: $1A_{1g}$ and $3E_g$.^{8,9} At room temperature, all these modes are located at low frequencies: 95 (E_g), 180 (A_{1g}), 300 (E_g), and 415 cm^{-1} (E_g). The modes at 95 and 415 cm^{-1} have a very weak intensity, and

their signal is lost when the sample is loaded into the DAC with the pressure medium. The other two modes show good signals, and their behavior was tracked precisely a few times. In the first run, we compressed the sample up to 30 GPa (Fig. 1a and b). The A_{1g} and E_g modes shift to higher frequencies intersecting each other at 13.3 GPa. The intensity does not change up to 17.95 GPa but follows a fast decrease afterward, vanishing completely at ~ 30 GPa. The pressure near 18 GPa coincides with a close-packed state and there are no signs of the symmetry change going further through “super-dense” packing. During this compression–decompression cycle, the sample retrieves the modes when it is released to ambient pressure. For the second run, we compressed the sample up to 60.98 GPa and found that after release, the high-pressure state is quenched (see Fig. 1c). The wide frequency release spectrum indicates a strong background, which is consistent with the amorphization indicated by the XRD measurements. Here, the feature marked as F_1 is out of the usual vibrational frequency range for fluoride compounds (0 – 700 cm^{-1}) but can be attributed to the presence of vanadium–oxygen or vanadium–hydroxide bonds, which are sometimes detected in VF_3 single crystals as impurities.⁹

Fig. 3 shows microscopic photographs of pressure-exposed VF_3 . A pressure of 43 GPa evidently had no effect on the released sample, while very strong changes in the form were observed when the sample was released from 61 GPa. The external changes are attributed to the amorphization described above and based on the XRD and Raman results. It is noticeable that the quenched amorphous material becomes one transparent unit instead of a loose powder. This transformation takes place regardless of hydrostatic compression, using gas as a medium, and nonhydrostatic compression, without any medium.

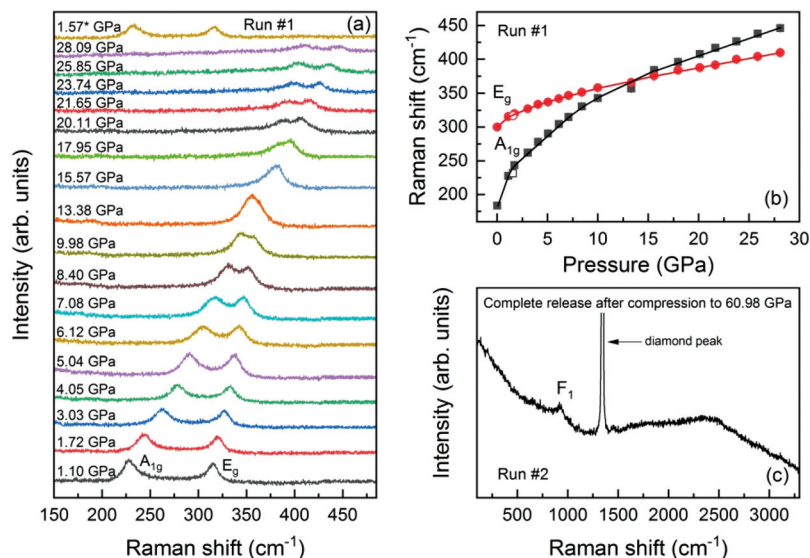


Fig. 2 High-pressure Raman spectra of VF_3 measured at room temperature. (a) Selected Raman spectra during the first compression cycle up to 30 GPa. (b) Pressure dependence of A_{1g} and E_g Raman modes. Here, filled symbols represent compression data, empty symbols are the release data. Solid lines are guides to the eye. (c) Raman spectrum of the released sample in a wide frequency range after the second compression cycle up to 60.98 GPa.

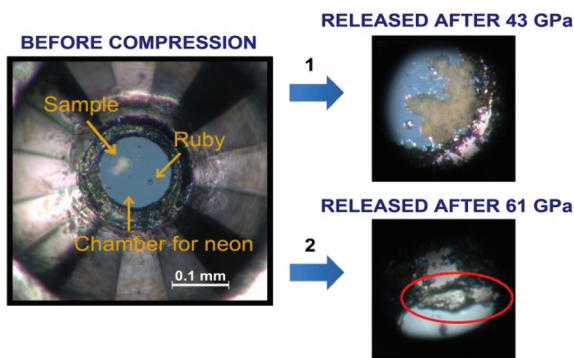


Fig. 3 Optical micrographs taken through a microscope before and after compression. The image on the left shows the initial layout in the compression chamber that is made in the Re gasket and placed on the diamond culet. Images on the right show the results of two separate compression–decompression cycles. (1) Sample released after compression to 43 GPa. No visible changes are observed, *i.e.*, the sample is a powder and no different from its starting condition. (2) Sample released after compression to 61 GPa. In this case, an obvious change in form is observed. The material, in turn, becomes one solid transparent glass-like piece. The red ellipse indicates its location. Note that the color of materials in the images provided may differ from the original because the reflections and the backlight give a different shade.

Solid-state amorphization for many systems can be understood in terms of the lowering of free energies of a high-density amorphous phase relative to a metastable lower density crystalline phase.^{25–28} Such a pressure-induced process in solid materials is less observed than the transition to the symmetric configuration because it involves a large number of disordered defects and distortions. Each case is quite specific

but is usually associated with pressure-induced structural deformations within the material. For instance, molecular crystals made of large clusters, such as fullerenes, sustain a collapse of their building blocks.²⁶ Oxides such as Y_2O_3 and Ta_2O_5 erode or lose connectivity between polyhedra.²⁷ Chalcogenides such as Ge–Sb–Te manifest atomic distortion toward disordered vacancies.²⁸ Meanwhile, in MF_3 fluorides (the case of FeF_3), the decisive factor is octahedral elongation, which results in substantial structural distortion.¹¹ Due to this reason, the structure of FeF_3 becomes dynamically unstable above 50 GPa suggesting a first-order phase transition at 51.1 GPa. However, to the best of our knowledge, quenchable states in MF_3 fluorides have not been observed to date.

To investigate the amorphization process in VF_3 , we performed lattice dynamics calculations. Fig. 4 shows the phonon dispersion curves along with the partial phonon densities of states (DOS) at different pressures. The phonon DOSs show the hybridization of V and F at low (<40 meV) and high (>60 meV) frequency range while the phonon modes dominated by F are observed in the middle frequency range of 40 and 60 meV, over the entire pressure range that was studied. Meanwhile, the phonon dispersion curves along the major symmetry directions of the Brillouin zone indicate the first sign of instability at 50 GPa – imaginary phonon frequency mode, so-called soft phonon mode, between F and T points in the Brillouin zone (see Fig. 4b). When the pressure increases further by 5 GPa, the soft phonon mode is observed at the F point (Fig. 4c and $S5^\dagger$). Similarly, phonon softening at $q = F$ for FeF_3 appears at 54.2 GPa, but in VF_3 , it manifests much more globally over the Brillouin zone (Fig. 4c and d). Multiple phonon mode softening could be the reason for the irreversible amorphization. However, in our case, the phonon softening modes are

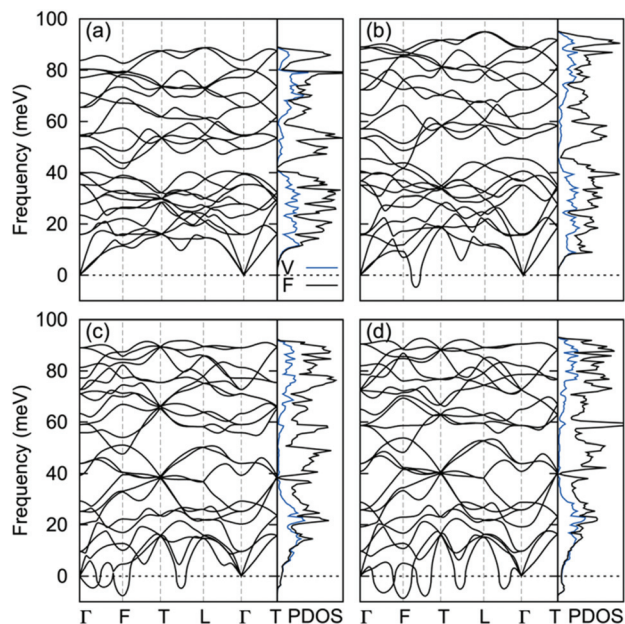


Fig. 4 Calculated phonon dispersion curves and corresponding partial phonon DOS at different pressures: (a) 30 GPa, (b) 50 GPa, (c) 55 GPa, and (d) 60 GPa.

observed at one exact point (F) and other non-exact points through the Brillouin zone. Therefore, we claim that the octahedral deformation with phonon softening at $q = F$ as shown in Fig. S5† is responsible for the amorphization process. This also suggests that other trifluorides, such as FeF_3 , may reveal amorphization quenched at sufficient pressure; otherwise, VF_3 will remain a peculiar representative of quenched amorphization.

Conclusions

The structure of rhombohedral VF_3 was studied under high pressure. At low pressures, volume reduction is achieved through coupled rotations of the VF_6 octahedra, which show modest strain resulting in a noticeable increase of the lattice parameter c at 4.95 GPa. Compression at higher pressures up to ~ 25 GPa is entirely achieved through the coupled rotation of VF_6 , which reduces the volume of the cuboctahedral voids. With reference to the F atom x coordinate dependence on the axial c/a ratio, we discern different sphere packing levels of type $8/3/c^2$. The increase of c/a is restrained in the range of 18–30 GPa and reaches its highest point, after which a “superdense” sphere packing inhibits VF_6 rotation and initiates its uniaxial deformation. For this reason, the rhombohedral phase becomes unstable. As there are no changes in the symmetry, the structure gradually proceeds to the amorphous state. Furthermore, this state can be quenched when a pressure of 56.7 GPa or higher is reached. A transparent, glass-like appearance of the material was observed when returned to ambient conditions. The stability of VF_3 is elucidated through

the analysis of vibrational properties. The phonon soft modes with increasing pressure from 50 to 60 GPa, particularly at the F point of the Brillouin zone, agree with our experimental results. Therefore, it can be concluded that the deformation of VF_6 plays a major role in VF_3 amorphization. Overall, the transition can be considered as having a very high-energy barrier and may be further tested in more detail, such as octahedral collapse using the pair distribution function technique.

Author contributions

The manuscript was written through contributions of all authors.

Conflicts of interest

The authors declare no conflict of interest.

Acknowledgements

Y. D and H.-k. M. acknowledge the support from National Key Research and Development Program of China 2018YFA0305703, Science Challenge Project, No. TZ2016001 and the National Natural Science Foundation of China (NSFC): U1930401, 11874075. S. K. acknowledges support from the NRF [grant no. NRF-2019R1F1A1052026] and KISTI Supercomputing Center [project no. KSC-2019-CRE-0172]. The XRD measurements at SPring-8 were carried out under the proposals of 2018A4140 and 2019A4131.

References

- 1 B. E. Douglas and S.-M. Ho, *Structure and Chemistry of Crystalline Solids*, Springer, New York, 2007. ISBN 0-387-26147-8.
- 2 H. Sowa and H. Ahsbahr, Pressure-Induced Octahedron Strain in VF_3 -type Compounds, *Acta Crystallogr., Sect. B: Struct. Sci.*, 1998, **54**, 578–584.
- 3 J.-E. Jørgensen, J. Staun Olsen and L. Gerwar, Compression mechanism of GaF_3 and FeF_3 : a high-pressure X-ray diffraction study, *High Pressure Res.*, 2010, **30**, 634–642.
- 4 P. Mondal, D. Opalka, L. V. Poluyanov and W. Domcke, Ab initio study of dynamical $E \times e$ Jahn-Teller and spin-orbit coupling effects in the transition-metal trifluorides TiF_3 , CrF_3 , and NiF_3 , *J. Chem. Phys.*, 2012, **136**, 084308.
- 5 P. Mondal, D. Opalka, L. V. Poluyanov and W. Domcke, Jahn-Teller and spin-orbit coupling effects in transition-metal trifluorides, *Chem. Phys.*, 2011, **387**, 56–65.
- 6 V. G. Solomonik, J. E. Boggs and J. F. Stanton, Jahn-Teller Effect in VF_3 , *J. Phys. Chem. A*, 1999, **103**, 838–840.
- 7 A. Corrales-Salazar, R. T. Brierley, P. B. Littlewood and G. G. Guzmán-Verri, Landau theory and giant room-temp-

- erature barocaloric effect in MF_3 metal trifluorides, *Phys. Rev. Mater.*, 2017, **1**, 053601.
- 8 P. Daniel, A. Bulou, M. Rousseau, J. Nouet and M. Leblanc, Raman-scattering study of crystallized MF_3 compounds ($M=Al, Cr, Ga, V, Fe, In$): An approach to the short-range-order force constants, *Phys. Rev. B: Condens. Matter Mater. Phys.*, 1990, **42**, 10545.
- 9 P. Daniel, A. Bulou, M. Leblanc, M. Rousseau and J. Nouet, Structural and vibrational study of VF_3 , *Mater. Res. Bull.*, 1990, **25**, 413–420.
- 10 A. H. Reshak, Revealing the influence of the compression mechanism on the electronic structure and the related properties of CrF_3 , *J. Alloys Compd.*, 2016, **660**, 1–10.
- 11 F. Zhu, X. Lai, X. Wu, Y. Li and S. Qin, Experimental and theoretical investigation on the compression mechanism of FeF_3 up to 62.0 GPa, *Acta Crystallogr., Sect. B: Struct. Sci., Cryst. Eng. Mater.*, 2014, **70**, 801–808.
- 12 R. Jia, C. G. Shao, L. Su, D. H. Huang, X. R. Liu and S. M. Hong, Rapid compression induced solidification of bulk amorphous sulfur, *J. Phys. D: Appl. Phys.*, 2007, **40**, 3763–3766.
- 13 H. K. Mao, X. Chen, Y. Ding, B. Li and L. Wang, Solids, liquids, and gases under high pressure, *Rev. Mod. Phys.*, 2018, **90**, 015007.
- 14 H. K. Mao, J. Xu and P. M. Bell, Calibration of the Ruby Pressure Gauge to 800 kbar Under Quasi-Hydrostatic Conditions, *J. Geophys. Res.*, 1986, **91**, 4673–4676.
- 15 Y. Seto, D. Nishio-Hamane, T. Nagai and N. Sata, Development of a Software Suite on X-ray Diffraction Experiments, *Rev. High Pressure Sci. Technol.*, 2010, **20**, 269–276.
- 16 A. Altomare, N. Corriero, C. Cuocci, A. Falcicchio, A. Moliterni and R. Rizzi, EXPO software for solving crystal structures by powder diffraction data: methods and application, *Cryst. Res. Technol.*, 2015, **50**, 737–742.
- 17 G. Kresse and J. Furthmüller, Efficient iterative schemes for *ab initio* total-energy calculations using a plane-wave basis set, *Phys. Rev. B: Condens. Matter Mater. Phys.*, 1996, **54**, 11169–11186.
- 18 S. Mattsson and B. Paulus, Density Functional Theory Calculations of Structural, Electronic, and Magnetic Properties of the 3d Metal Trifluorides MF_3 ($M = Ti-Ni$) in the Solid State, *J. Comput. Chem.*, 2019, **40**, 1190–1197.
- 19 J. P. Perdew, K. Burke and M. Ernzerhof, Generalized Gradient Approximation Made Simple, *Phys. Rev. Lett.*, 1996, **77**, 3865.
- 20 A. Togo and I. Tanaka, First principles phonon calculations in materials science, *Scr. Mater.*, 2015, **108**, 1–5.
- 21 J.-E. Jørgensen, W. G. Marshall and R. I. Smith, The compression mechanism of CrF_3 , *Acta Crystallogr., Sect. B: Struct. Sci.*, 2004, **60**, 669–673.
- 22 J.-E. Jørgensen and R. I. Smith, On the compression mechanism of FeF_3 , *Acta Crystallogr., Sect. B: Struct. Sci.*, 2006, **62**, 987–992.
- 23 O. L. Anderson and J. E. Nafe, Bulk modulus-volume relationship for oxide compounds and related geophysical problem, *J. Geophys. Res.*, 1965, **70**, 3951–3963.
- 24 S. Usha Devi and A. K. Singh, Volume compression of $CuCl$ to 7 GPa, *Pramina*, 1981, **17**, 461–468.
- 25 R. J. Hemley, A. P. Jephcoat, H. K. Mao, L. C. Ming and M. H. Manghnani, Pressure-induced amorphization of crystalline silica, *Nature*, 1988, **334**, 52–54.
- 26 B. Sundqvist, Fullerenes under high pressure, *Adv. Phys.*, 1999, **48**, 1–134.
- 27 L. Wang, W. Yang, Y. Ding, Y. Ren, S. Xiao, B. Liu, S. V. Sinogeikin, Y. Meng, D. J. Gosztola, G. Shen, R. J. Hemley, W. L. Mao and H. K. Mao, Size-Dependent Amorphization of Nanoscale Y_2O_3 at High Pressure, *Phys. Rev. Lett.*, 2010, **105**, 095701.
- 28 S. Caravati, M. Bernasconi, T. D. Kühne, M. Krack and M. Parrinello, Unravelling the mechanism of pressure induced amorphization of phase change materials, *Phys. Rev. Lett.*, 2009, **102**, 205502.